Langmuir

Article

pubs.acs.org/Langmuir

Self-Assembly and Emulsification of Poly{[styrene-*alt*-maleic acid]-*co*-[styrene-*alt*-(*N*-3,4-dihydroxyphenylethyl-maleamic acid)]}

Yi Chenglin,[†] Yang Yiqun,[†] Zhu Ye,[†] Liu Na,[†] Liu Xiaoya,*[,†] Luo Jing,[†] and Jiang Ming[‡]

[†]Key Laboratory of Food Colloids and Biotechnology, Ministry of Education, School of Chemical and Material Engineering, Jiangnan University, Wuxi 214122, China

[‡]Key Laboratory for Molecular Engineering of Polymers, Ministry of Education; Department of Macromolecular Science, Fudan University, Shanghai 200433, P. R. China

Supporting Information

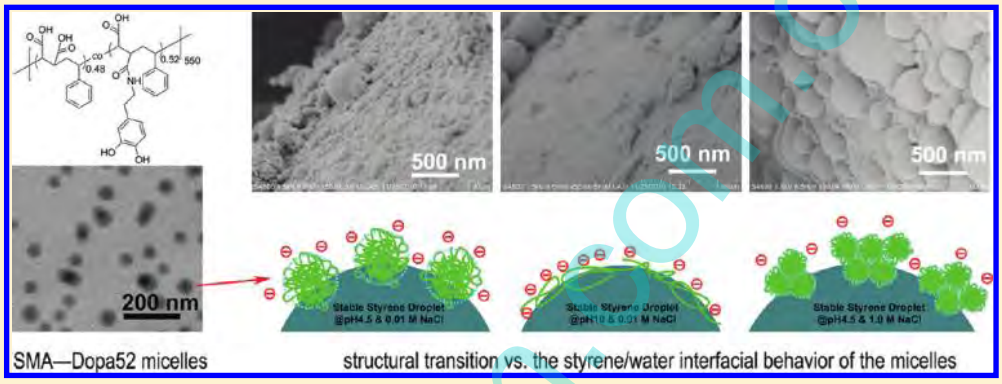

ABSTRACT: Self-assembled polymeric micelles can be used as efficient particulate emulsifiers. To explore the relationship between the structure and the oil−water interfacial behavior of the micelle emulsifiers, a new type of amphiphilic random copolymer, poly{(styrene-*alt*-maleic acid)-*co*-[styrene-*alt*-(*N*-3,4-dihydroxyphenylethyl-maleamic acid)]} (SMA−Dopa), was synthesized, self-assembled into micelles, and used as emulsifiers. SMA−Dopa was synthesized via an aminolysis reaction between dopamine and commercial alternating copolymer poly(styrene-*alt*-maleic anhydride) (SMA). Dopamine moiety facilitated the self-assembly of the SMA−Dopa in selective-solvent into stable micelles, and increased the adsorption of the SMA−Dopa at the oil−water interface. Additionally, the structural transition of the self-assembled SMA−Dopa52 micelles in response to pH and salinity changes were confirmed by means of TEM, AFM, DLS, aqueous electrophoresis techniques, potentiometric titration, and pyrene fluorescence probe methods. Micelles shrunk with increasing salinity, and flocculation of the shrunken primary micelles occurred at salt concentration exceeding 0.1 M. The micelles swelled with increasing pH, and the disassociation of the SMA−Dopa52 micelles occurred at pH above approximately 6.5. The structure of the micelles plays a crucial role in the oil−water interfacial performance. Micelles with various structures were used as emulsifiers to adsorb at the styrene−water and toluene−water interfaces. The emulsifying characteristics demonstrated that self-assembled SMA−Dopa52 micelles with moderately swollen structure (at 2 < pH < 6) combine the advantages of the solid particulate emulsifiers and polymeric surfactants, possessing excellent emulsifying efficiency and good emulsion stability. Moreover, the emulsifying performance of the SMA−Dopa52 micelles could be enhanced by the addition of salt.

1. INTRODUCTION

Amphiphilic copolymer self-assembled micelles of various morphologies, including spheres, rods, bowls, and vesicles, have attracted much attention in the past decade.[1−7] These polymeric micelles can be useful in many potential applications, such as drug delivery,[8−11] nanocontainers,[12] catalysts,[13] sensors,[14−16] and others.[17] The inherent and robust properties of polymeric micelles, which result from their fascinating structures and/or nanoscale effects, have contributed to their extensive potential applications. For example, polymer vesicles can be used as drug carriers due to their high encapsulation efficiency. Additionally, some polymeric micelles are surface-active, as reported in the pioneering work of Fujii et al.[18] They showed that self-assembled micelles based on an ABC triblock copolymer could be used as novel efficient particulate emulsifiers and stabilized 1-undecanol-in-water emulsion possessing pH-responsiveness. Because amphiphilic random or alternating copolymers are much easier to synthesize and because of their abilities to self-assemble into micelles with various structures and properties,[2,5,19,20] random copolymer P(St-*alt*-MAn)-*co*-P(VM-*alt*-MAn) self-assembled micelles were photo-cross-linked and used as a particulate emulsifier

Received: July 25, 2011
Revised: May 27, 2012
Published: May 28, 2012

dx.doi.org/10.1021/la301605a | *Langmuir* 2012, 28, 9211−9222

in one of our previous reports.[21] We found that cross-linked micelles had extremely high emulsifying efficiency, with micelle concentrations as low as 1.5 mg·mL^{-1}, being sufficient to stabilize emulsions for many months. However, the underlying principles of the high emulsifying efficiency of self-assembled polymeric micelles are still not fully understood.

The colloidal particles used to prepare and stabilize emulsions, so-called "Pickering" or "Ramsden" emulsions,[22,23] are particulate emulsifiers that adsorb at oil−water interface and have caused a resurgence of interest in a wide range of applications, including medical uses,[24] personal care products, food products,[25] catalysts,[26] and fabrication of new materials.[27,28] Various types of colloidal particles have been used as particulate emulsifiers, such as inorganic particles,[29] polymer-grafted inorganic nanoparticles,[30−33] organic latexes,[27,34−39] microgels,[40−42] and self-assembly micelles.[18,21] Pickering emulsions are often distinguished by their excellent stability and high discontinuous phase volume fractions over conventional emulsions stabilized by surfactants.[43,44] Additionally, particulate emulsifiers offer more reproducible formulations, reduced foaming problems, and lower toxicity profiles compared to conventional surfactants.[43,44]

The fabrication of high-efficiency particulate emulsifiers and the elucidation of their mechanism would be valuable. Generally, polymeric particles possess better fabrication tailorability and higher emulsification efficiency than inorganic particles, and they have attracted much attention over the past decade. Examples include silica nanoparticles grafted with different kinds of polymer brushes,[30−33] sterically stabilized latex particles,[27,34−39] and lightly cross-linked microgels.[35,40−42,45−47] The high emulsification efficiency and stimulus responsiveness are attributed to the design of the swelling polymer chains or segments on the surface of those particulate emulsifiers. Does this principle also govern the case of the self-assembled micelles based on amphiphilic random/alternating copolymers? In addition to the influence of the swelling polymer chains, simultaneous structural transformations also play an important role in the emulsification performance of most polymeric emulsifiers. Considering that polymer micelles possess better structural control and tailoring capabilities relative to particles prepared by other methods,[4,5] polymeric micelles appear to be good model particulate emulsifiers to elucidate the relationship between the structure and emulsification performance of most polymer particulate emulsifiers. In this article, the structure of the self-assembled micelles is manipulated in two normal respects: the chemical structure of the amphiphilic copolymer and simple environmental stimuli (pH and/or salt), which, in turn, influence their emulsifying performance.

Poly(styrene-*alt*-maleic anhydride) (SMA) is a commercially available alternating copolymer with a hydrophobic monomer, styrene, and a hydrophilic monomer, maleic anhydride. The distinctive sequence and composition impart unusual properties to the polymer, which have generated interest in a wide range of scientific fields, such as nanotechnology,[48−51] drug delivery,[52,53] and the pulp and paper industry as a surface sizing agent for paper products. Given that highly charged hydrolyzed SMA (HSMA) is a conventional polymeric surfactant, self-assembled micelles based on the HSMA could be good candidates to illuminate the influence of the structure on the emulsification performance of polymer particulate emulsifiers and to bridge the polymeric surfactants and particulate emulsifiers, which may contribute to an increased understanding in challenging areas where the polymeric surfactants and particulate emulsifiers cooperate,[54,55] such as cosmetic and food industries. However, according to the research of T. G. M. van de Ven and co-workers,[56−60] it is hard to get stable aggregates based on HSMA with relatively low molecule weight, except when the pH of the solution is near 7. There is also a question as to whether the stable aggregates formed at pH 7 will retain their stable structure when aggregates migrate from solution onto the oil−water interface. Increasing molecule weight and slightly hydrophobic modification may be able to tackle this problem by facilitating the self-assembly of polymers into micelles with stable structures both in solution and at the oil−water interface, thereby retaining the ability to disassociate from intact micelles into polymeric surfactants in response to a simple change in pH.

Recently, 3,4-dihydroxy-L-phenylalanine (DOPA) has been found in mussel specialized adhesive proteins and has attracted much attention owing to the amazing ability of mussels to adhere to various kinds of surfaces.[61] Previous research work has shown that the catechol groups in DOPA and its analogue dopamine are capable of forming strong bonds with various inorganic/organic substrate surfaces, and these bonds were shown to be stronger than biotin−streptavidin interactions.[61−63] In 2007, Lee et al. used dopamine self-polymerization as a powerful approach for applying multifunctional coatings onto many surfaces, including noble metals, metal oxides, ceramics, and polymers, by mimicking MAPs.[61] Although the dopamine moiety has excellent solid surficial adhesion property,[64−67] no attention has been focused on the amphiphilicity of the catechol groups or its liquid−liquid interfacial behavior.

In this study, dopamine-modified HSMA (SMA-Dopa) with relatively high molecular weight was designed and synthesized by aminolysis of SMA with dopamine and the hydrolysis of the residual malic anhydride groups, and then self-assembled into polymer micelles. The emulsifying characteristics of the micelles will be reported to illuminate the relationship between the micellar structure and the interfacial properties. The structure of SMA-Dopa self-assembled micelles is innately dependent on the chemical structure of the amphiphilic copolymers and postnatally manipulated by environmental stimulus changes, such as pH and salinity. Our work will show how the chemical structure of the polymer and changes in environmental stimulus affect the micellar structure and in turn influence the emulsification performance.

2. EXPERIMENTAL DETAILS

2.1. Materials. Styrene (St, Sinopharm Chemical Reagent Co., Ltd., SCRC) was dried with CaH_2 for 24 h, distilled under reduced pressure, and then stored at 5 °C prior to use. Styrene−oil phase polymerization was initiated with V65 (2,2′-azobis(2,4-dimethyl valeronitrile)) which was a gift from Qingdao Runxing Photoelectric Material Co. (LTD, Qingdao, China). Water was first deionized by reverse osmosis and purified to a resistivity of 18.2 MΩ·cm using a Millipore water purification system. Other reagents were used as received.

In the present study, poly{(styrene-*alt*-maleic acid)-*co*-[styrene-*alt*-(*N*-3, 4-dihydroxyphenylethyl-maleamic acid)]} (SMA−Dopa), were prepared by the aminolysis reaction between the alternating copolymer SMA and dopamine. The preparation and characterization details are provided in the Supporting Information (SI). The chemical structure of the amphiphilic random copolymers is illustrated in Figure 1. The degrees of aminolysis (α) of the SMA−Dopa samples used in this study were 0 (SMA−Dopa0), 27% (SMA−Dopa27), and 52%

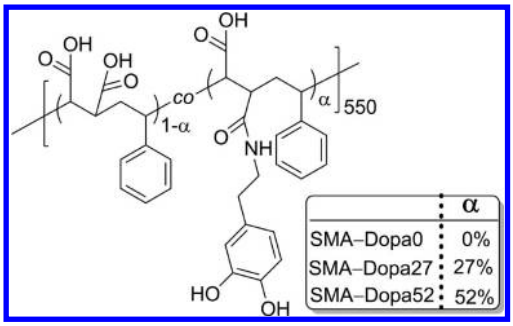

Figure 1. Chemical structure of the amphiphilic copolymer SMA–Dopa used in the present study. The parameters of the polymers were determined by GPC and ^{1}H NMR.

(SMA–Dopa52), respectively; α is defined as the percentage of the structural units bearing dopamine among the total anhydride units.

2.2. Preparation of SMA–Dopa Micelles. Micelles were prepared by a self-assembly method similar to those used by Eisenberg et al. for preparing "crew-cut" micelles from amphiphilic block copolymers.[1,7] The polymers were dissolved in *N*,*N*-dimethyl formamide (DMF) to form 20 mg·mL^{-1} solutions that were stirred overnight. To induce self-assembly, water was added dropwise into the solutions at a rate of 0.2 wt % per minute to the desired water content. The solutions were stirred for 3 h and were then quenched into an excess of water before they were dialyzed against water to remove the remaining DMF.

2.3. Characterization of the Micelles. *Transmission Electron Microscopy (TEM).* TEM images of the particles were obtained on a JEOL JEM-2100 (HR) LaB6 transmission electron microscope at a 200 kV accelerating voltage. The TEM samples were prepared by dropping diluted micelle solutions onto copper grids coated with a thin polymer film and then drying them at room temperature without any further staining treatment. Before visualization under TEM, samples were further dried under infrared lamp. The size and size distribution of the particles were estimated with *Image-Pro Plus 5.1* software (Media Cybernetics).

Atomic Force Microscopy (AFM). Sample for the AFM measurements was prepared by casting the micelles solution on clean mica and drying them in a constant-humidity oven at 30 °C for 24 h. The AFM was performed on a CSPM3300 (Benyuan Co.) with a vertical resolution of 0.1 nm and a horizontal resolution of 0.2 nm. The instrument was operated in contact mode during this study, and the scanning range was set at 5.0 μm × 5.0 μm.

Zeta Potential and Average Diameter. SMA–Dopa micelles were characterized for size and zeta potential (ζ) using dynamic light scattering (DLS) and electrophoretic mobility measurements, both of which were conducted with a combination BIC 90Plus and ZetaPALS instrument (Brookhaven Instruments Corp., USA). The size of the micelles was measured in triplicate and expressed as the average ± standard error. Prior to the measurement of the micelle size in response to pH changes, the samples were filtered through 0.45 μm Millipore filters (hydrophilic Millex-LCR, PTFE). The zeta potential was calculated from the electrophoretic mobility (u) using the Smoluchowski relationship, $\zeta = \eta u/\varepsilon$, under the assumption that $\kappa\alpha \ll 1$, where η is the solution viscosity, ε the dielectric constant of the medium, and κ and α are the Debye–Hückel parameter and the particle radius, respectively. Zeta potentials were averaged over 20 runs.

To further determine the size distribution of SMA–Dopa micelles at various pHs, dynamic light scattering (DLS) were carried out again using an ALV-5000 laser light scattering spectrometer. All the solutions were filtered through 0.45 μm Millipore filters to remove dust and then kept at 25 °C for at least 2 h before light scattering measurements. DLS measurements were performed at a fixed scattering angle of 90°.

Fluorescence Pyrene Probe Method. Steady-state fluorescence spectra of pyrene were recorded with a Shimadzu RF-5301PC spectrometer using a thermostatted cell. The typical pyrene monomer fluorescence spectra were observed by excitation at 335 nm (excitation slit width: 3 nm; emission slit width: 3 nm). The spectra were used to determine the ratios (I_1/I_3) of the fluorescence intensities of the first (I_1, 373 nm) and third (I_3, 384 nm) vibronic peaks of monomeric pyrene. The ratio I_1/I_3 is known to be an excellent index of the effective polarity in the probe microenvironment.[68] All experiments were performed at 25 °C.

In the first stage of the preparation of the sample solutions, a saturated pyrene-probe aqueous solution of approximately 6.0 × 10^{-7} M at 25 °C was obtained according to the method reported in the literature.[69] Then, a precise 0.5 mL saturated pyrene aqueous solution was added into 8 mL of SMA–Dopa52 micelles solution with concentration of 1.0 mg·mL^{-1} at different pH or salinity. Each sample was under stirring for 24 h at 25 °C prior to use.

2.4. IFT Measurement. The interfacial tension (IFT) measurements were carried out on an OCA40 (DataPhysics Instruments GmbH) equipped with a pendant drop module. The picture analysis was done with the help of the Drop Shape Analysis program supplied by the manufacturer. Each pendant drop of micelle solution was immersed in toluene in a quartz cuvette and aged for 0.5 h at temperature of 25 °C. The IFT of the pure toluene–water interface was determined to be 36 mN·m^{-1} prior to measurement.

2.5. Emulsion Preparation and Characterization. *Emulsion Preparation.* Equal volumes of oil (toluene or styrene) and an aqueous solution of SMA–Dopa micelles (with a polymer concentration of 2 mg·mL^{-1}) at various pHs or salt concentrations were placed in glass vessels at room temperature. The mixtures were kept in a thermostatted bath at 25 °C for 10 min and then homogenized at 5000 rpm for 2 min by a XHF-D H-speed dispersator homogenizer (1 cm head) at 25 °C. The type of all emulsions was O/W, determined by a drop test as well as conductivity measurement. The emulsions were sealed and placed under quiescence condition at room temperature after homogenization.

Light Microscopy. Emulsion droplets were imaged with an optical microscope (DM-BA450, Motic China Group Co., LTD) fitted with a digital camera after a 1: 6 dilution in the continuous-phase liquid for better optical clarity. Droplet diameter was measured by image analysis using the *Motic Images Advanced* software. The statistical analysis of the droplet size was performed and expressed as the average ± the standard error.

2.6. Scanning Electron Microscopy (SEM). Because of toluene volatility, the emulsions formed could not be introduced into the SEM chamber. An oil-phase solidification method was used to visualize the morphologies of SMA–Dopa in the oil–water interface. The method is similar to the previous report,[21,70] with some modifications. Styrene with 2.0 mol % V65 in place of toluene was used as the oil phase to prepare emulsions with equal volume of water (3 mL/3 mL) using SMA–Dopa as the emulsifier at various pH levels or salt concentrations, the micelle solution was 2 mg·mL^{-1}. The product emulsions homogenized at 5000 rpm for 2 min were polymerized at 65 °C for 24 h under quiescence conditions. The emulsion droplets with SMA–Dopa on the surface slowly solidified. The resultants were collected and washed by centrifugation and dried at 35 °C under vacuum for 48 h. The dried droplets were placed on a copper stub and sputter-coated with thin layers of gold, and then observed with a Quanta-200 field-emission microscope that was operated at an accelerating voltage of 20 kV.

3. RESULTS AND DISCUSSION

The chemical composition and structural parameters of the amphiphilic alternating copolymer SMA–Dopa used in this study are illustrated in Figure 1. The structural unit number, 550, calculated according to the molecular weight of precursor polymer SMA, indicates that the SMA–Dopa chains are sufficiently long to associate and aggregate into colloidal particles. The increasing degree of aminolysis (α) enhances the amphiphilicity of the polymer, in turn, decreasing the

dx.doi.org/10.1021/la301605a | *Langmuir* 2012, 28, 9211–9222

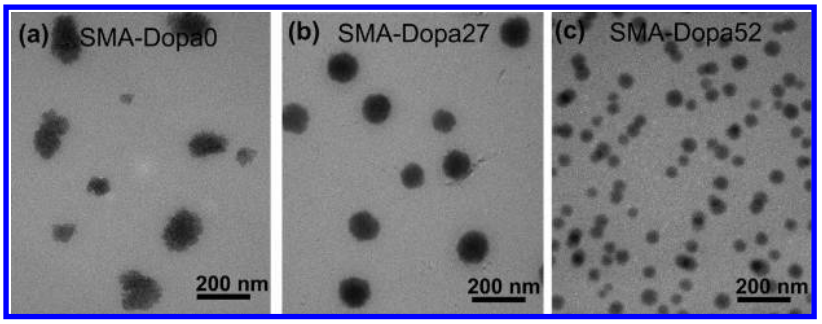

Figure 2. TEM images of (a) SMA−Dopa0 aggregates, (b) SMA−Dopa27 micelles, and (c) SMA−Dopa52 micelles. The mass concentration was 0.15 mg·mL^{-1}.

homogeneity of the strictly alternating copolymer SMA−Dopa0, namely, HSMA.

3.1. Self-Assembly of SMA−Dopa. The selective-solvent method[1] reported by Eisenberg was chosen to prepare the SMA−Dopa micelles. Figure 2 shows the morphologies of the SMA−Dopa micelles. The SMA−Dopa0 aggregates appear irregular with many nanopapillas on their surface. It seems likely that the strictly alternating copolymer SMA−Dopa0 could not self-assemble well because of the reduced asymmetry in amphiphilicity of the copolymer. It coincides with the reports by T. G. M. van de Ven et al.[56−60] The irregular aggregates formed also indicate that the SMA−Dopa0 tends toward association, probably due to the sufficiently long chains. As a comparison, SMA−Dopa27 and SMA−Dopa52 could aggregate into regular sphere micelles, as shown in Figure 2b and c. Recall that, in the chemical structure of SMA−Dopa in Figure 1, the slightly hydrophobic dopamine moieties bestow asymmetry on the homogeneous alternating copolymer SMA−Dopa0 and enhance the amphiphilicity of the polymers, SMA−Dopa27 and SMA−Dopa52. That asymmetry and amphiphilicity benefit not only the self-assembly of SMA−Dopa ($\alpha > 0$) into micelles primarily by hydrophobic interactions but also the structural stability of the formed micelles. Hence, in present study, the SMA−Dopa52 micelles might be the most suitable candidate for the following study owing to the probable structural transition of the micelles from stable micelles to an extremely swollen state or even disassembled free polymers chains in response to changes in pH. The size of the SMA−Dopa52 micelles (d = 55.7 ± 9.4 nm) is smaller than that of SMA−Dopa27 (d = 102 ± 23 nm), as can be observed by comparing the morphology in Figure 2b with that of Figure 2c. The reason is still not clear.

To further study the structural stability of the SMA−Dopa52 micelles, micelle solutions were casted on the mica and observed by AFM, as shown in Figure 3a and b. The strong attraction between the polar groups of the polymers, and the mica substrate has been demonstrated.[71] According to statistical analysis of the SMA−Dopa52 micelles in Figure 3c, the micelles became deformed, with a mean diameter of 77.8 nm and a mean height of 27.5 nm, due to the attraction between the mica substrate and the micelles. The spherical structure of the micelles could still be distinguished, indicating the stability of the micellar structure. As a comparison, the hydrodynamic diameter of SMA−Dopa52 micelles was carefully measured at a scattering angle of 90° with a diluted solution at pH 3.8 without salt. The size of the micelles as determined by DLS (D_h = 152 nm) was larger than that by TEM and AFM, as shown in Figure 3c and d, suggesting the swollen structure of micelles in aqueous solution.

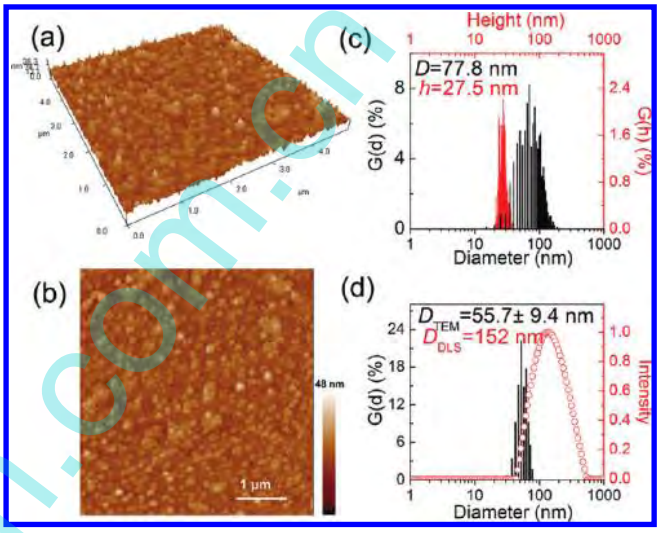

Figure 3. AFM images of the SMA−Dopa52 micelles. The mass concentrations 0.5 mg·mL^{-1}. Key: (a) surface plot, (b) top view, and (c) diameter and height analysis of the micelles as observed by AFM image b. As a comparison, (d) the statistical size distribution, counted from more than 500 spheres by TEM, as well as the size distribution determined by the ALV-5000 laser light scattering spectrometer.

3.2. Interfacial Property of Dopamine Moieties. Regarding the benefit of dopamine moieties on the self-assembly process of the polymers, as described above, we wondered if there was any further influence on the oil−water interfacial performance. SMA−Dopa0 and SMA−Dopa52 micelles were used as emulsifiers to stabilize toluene-in-water emulsions. Given that deprotonated HSMA is a conventional polymeric surfactant, to highlight the influence of the dopamine moiety, the concentrations of the emulsifiers were both lowered to 0.5 mg·mL^{-1} at pH 3.8, and the appearance of the emulsions one day after homogenization is shown in Figure 4a. There is about 30 vol % oil separated in the emulsion stabilized by SMA−Dopa0, accompanied with a broader size distribution of the emulsion droplets relative to SMA−Dopa52 (see Figure 4b and c), indicating that the dopamine moiety significantly improves the emulsifying performance of HSMA. To prove that the tensioactivity of the dopamine moiety grafted to SMA−Dopa in the toluene-in-water emulsion system is not a special case, a dopamine-modified hyaluronic acid (HA-DN) that has been previously synthesized to immobilize on magnetite nanocrystal surfaces by Lee at al.[63] was chosen and used as an emulsifier to stabilize petrolatum oil-in-water emulsions and compared with hyaluronic acid in SI. Figure S6 shows that dopamine remarkably improved the emulsification performance

dx.doi.org/10.1021/la301605a | Langmuir 2012, 28, 9211−9222

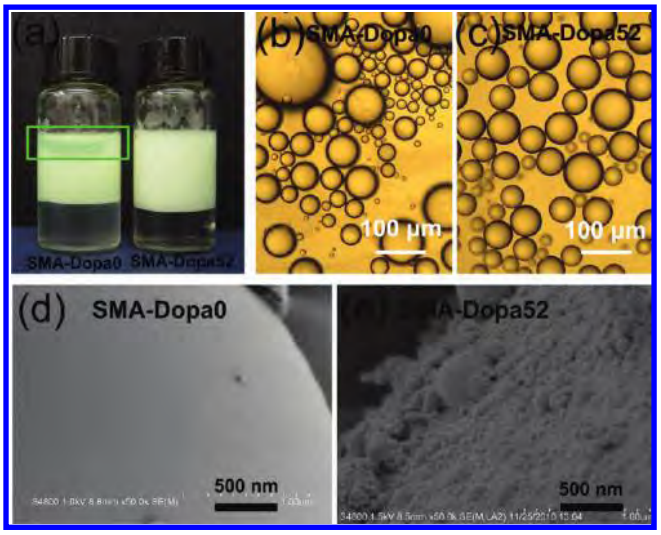

Figure 4. Influence of dopamine on the emulsification performance of SMA−Dopa. (a) Appearance of the toluene-in-water emulsions stabilized by SMA−Dopa0 (left) and SMA−Dopa52 (right). The concentrations of the polymer aqueous solutions were 0.5 mg·mL^{-1}, with no salt at pH 3.8. Equal volumes of polymer aqueous solutions and toluene were homogenized at 5000 rpm for 2 min, the toluene containing 0.05 wt % Solvent Yellow 43 (CAS no.: 19125−99−6). The green pane highlights the separated toluene, ca. 30 vol %. (b,c) Optical micrographs of the emulsions from (a). Scanning electron micrographs of styrene-in-water emulsions stabilized by (d) SMA−Dopa0 and (e) SMA−Dopa52 and polymerized using a V65 initiator. The mass concentrations of the polymer solutions were 2 mg·mL^{-1} with 10 mM NaCl at pH 4.5.

of HA-DN relative to HA (i.e., the dopamine moiety could stably adsorb at the oil−water interface). Considering the biocompatibility and moisture retention of HA, an added tensioactivity will offer HA-DN greater applications in the cosmetic, medicine, and food industries.

To further investigate the influence of the dopamine moiety on the micellar interfacial properties, toluene was replaced by styrene (containing initiator V65) to prepare styrene-in-water emulsions; it was then polymerized, and the surface morphologies of the polymerized polystyrene (PS) beads were examined by SEM.[21,70] Figure 4d shows a smooth surface of one PS bead where the styrene-in-water interface was stabilized by SMA−Dopa0 at pH 4.5 with 10 mM NaCl in solution. The smooth surface indicates that SMA−Dopa0 adsorbed at the styrene-in-water interface as a conventional polymeric surfactant without aggregating or associating. We postulate that the association between SMA−Dopa0 segments is resolved and destroyed by the oil phase styrene. As a comparison, Figure 4e shows the rough surface of a styrene-in-water interface stabilized by SMA−Dopa52 micelles at pH 4.5, indicating that SMA−Dopa52 micelles can remain intact and adsorb as a typical particulate emulsifier. The details will be discussed further in Figure 10. The good structural stability of SMA−Dopa52 micelles at the oil−water interfaces brought about by dopamine moieties benefits not only the emulsification performance, but also the structural transition capabilities of the micelles.

3.3. Structural Transition of SMA−Dopa52 Micelles. The carboxyl groups of SMA−Dopa52 offer the self-assembled micelles the ability to respond to environmental stimuli such as pH and ionic strength (salinity). Similar responsiveness has been previously reported for numerous other polymer micelles. Prior to investigation of the influence of the micellar structural transition on the emulsification performance, it was necessary to grasp the responsiveness of SMA−Dopa52 micelles to pH and salinity changes.

Salinity. Figure 5a illustrates the zeta potential of SMA−Dopa52 micelles as a function of sodium chloride concentration

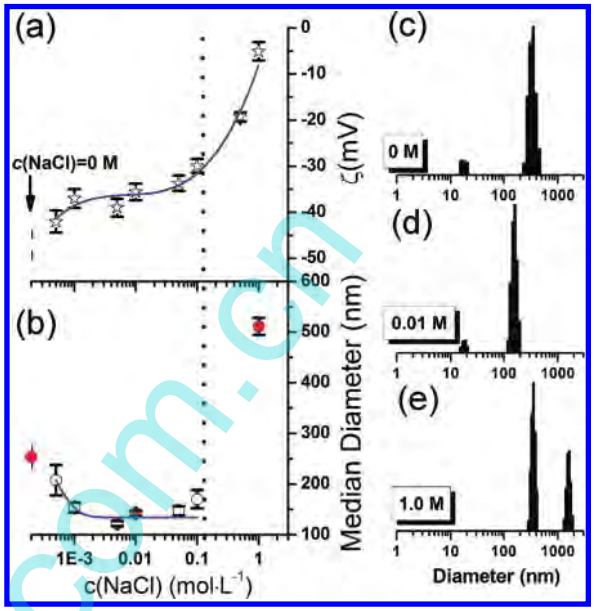

Figure 5. Influence of the salinity on the size (a) and zeta potential (b) of the SMA−Dopa52 micelles. The diameter distributions of SMA-Dopa52 micelles are shown for different salt concentrations: 0 M (c), 0.01 M (d), and 1.0 M (e). The mass concentration of the micelles was 0.5 mg·mL^{-1}, and all samples were at pH 4.5.

of the particle aqueous solutions, showing an inverse "S" curve. The curve indicates that there are two distinct impacts of increasing salinity over the entire range. One impact is that the electrostatic shielding effect brought about by the added salt, similar to what occurred with PNIPAm microgels with carboxyl groups reported by Ngai et al.,[46] resulted in an increase in the zeta potential from −47 mV to −30 mV with salinity increasing from 0 to 0.1 M. Another impact may be the flocculation of the micelles due to fewer electrostatic repulsive forces among the micelles brought about by higher concentrations of added salt, resulting in a dramatic increase in the apparent zeta potential to −5.1 mV.

The response of the micelle size to salinity changes, as shown in Figure 5b, provides further details on the structural transition. The micelle size decreases from 272 to 150 nm as the salinity increases to 0.1 M due to a decrease in the electrostatic repulsive forces among the polymer chains of the SMA−Dopa52 micelles. The abrupt increase in micelle size for salinities exceeding 0.1 M, indicates the flocculation of the shrunken primary micelles, as detailed in Figure 5c−e. There is a distinguished terrace over salinities ranging from 1 mM to 0.1 M, implying the slightly shrunken and stable structure of the SMA−Dopa52 micelles. Hence, 10 mM salt will be added into the micelle solutions when the pH influence is studied.

pH. To determine the structural transitions triggered by changes in pH, a potentiometric titration of an SMA−Dopa52 solution was performed, as shown in Figure S7 in SI. Recall the chemical structure of SMA−Dopa52, in addition to the original two pK_a values of HSMA, pK_{a1} = 4.4 and pK_{a2} = 10.3,[72] the

dx.doi.org/10.1021/la301605a | Langmuir 2012, 28, 9211−9222

dopamine moiety should bestow another pK_a on SMA–Dopa52 due to the catechol groups (pK_a = 9.4). There are only two distinct pK_a values for SMA–Dopa52: pK_{a1} = 4.6 and pK_{a2} = 9.9, as shown in Figure S7. There may be two explanations for this finding: (1) Attachment of dopamine moieties (α = 52%) not only decreases the dicarboxylic acid units (maleic acid), but also increases the monocarboxylic acid units (*N*-3,4-dihydroxyphenylethyl-maleamic acid), resulting in a slightly greater pK_{a1} value for SMA–Dopa52 than for HSMA. (2) The pK_a of the catechol groups and pK_{a2} of the residual carboxylic acid groups cannot be distinguished and appear as a mixed apparent pK_{a2} value of 9.9.

Figure 6a shows the influence of the pH on the size and zeta potential of the SMA–Dopa52 micelles. It is interesting to note

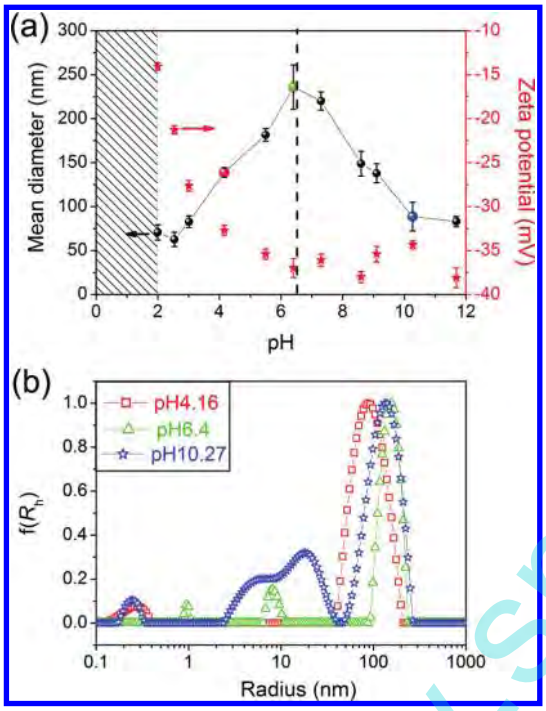

Figure 6. (a) Influence of the pH on the size (●) and zeta potential (★) of the SMA–Dopa52 micelles. The polymer mass concentration was 0.5 mg·mL^{-1} with 0.01 M NaCl in an aqueous dispersion. (b) The size distribution of the micelles at pH 4.16, 6.4, and 10.27, respectively, determined by an ALV-5000 laser light scattering spectrometer.

that there are two distinct trends in variation of the mean micelle size with increasing pH when the pH is above ca. 2.0. The maximum mean size lies at approximately pH 6.5. Note that the micelles are unstable to flocculation due to less repulsion forces among the micelles at pH < 2. When the pH is increased from 2.0 to 6.4, the enhanced electrostatic repulsion forces among the polymer chains of the micelles, brought about by an increased protonation of the carboxylic acid groups, results in a dramatic increase in micelle size from 70.7 ± 8.7 nm to 235.9 ± 25.4 nm. This swelling behavior of the micelles is caused by increased protonation and can further be supported by the decrease in zeta potential from −14 mV to −36 mV. A similar swelling behavior of polymeric particles responding to pH changes has been reported elsewhere.[73]

A pH 6.5 boundary may imply the full deprotonation of the primary carboxylic acid groups and the beginning of the deprotonation of residual neighboring carboxylic acids and catechol groups. Further increases in pH result in a decrease in micelle size and slight fluctuations in the zeta potential. This is probably due to the disassociation of the extremely swollen SMA–Dopa52 micelles triggered by further deprotonation of the residual carboxylic acid and catechol groups. Figure 6b shows the hydrodynamic radius distribution of the SMA–Dopa52 micelles at various pHs. The hydrodynamic radius distribution of the SMA–Dopa52 micelles are not monomodal distribution curves. At pH 10.27, there is a new isolated, broad, strong peak from 2 to 45 nm compared to that at pH 4.16 and 6.4, indicating that more small aggregates are disintegrated from larger aggregates. The disintegration of micelles may depend on having a sufficient enhanced electrostatic repulsion force and hydrophilic interaction provided by the progressive increase of deprotonated groups with weakened hydrophobic interaction. This phenomenon is governed by a general principle, as reported by Zhang et al.,[74,75] that the formation and stabilization of micelles is controlled by a delicate balance between the hydrophobic and hydrophilic interactions, with more hydrophilic groups stabilizing a larger total interfacial area generally leading to smaller particles.

Fluorescence Pyrene Probe Method. To further illuminate the structural transition of SMA–Dopa52 micelles in response to salinity and pH changes, a simple steady-state fluorescent pyrene probe method[69,76] was used to investigate the variation of the hydrophilic/hydrophobic microenvironment of the micelles. The pyrene probe is added to the micelle solutions at different pHs and salinities. The variation is described in terms of the ratio I_1/I_3: the intensities of the first and third bands, respectively, in the pyrene fluorescence emission spectrum. This ratio has been shown to be very sensitive to the polarity of its environment.[76] Under our experimental conditions, the I_1/I_3 values in water and pure styrene were 1.87 and 1.07, respectively.

Figure 7 shows the response of the I_1/I_3 to pH (●) and salinity (□) changes. As salinity increased from 0 to 1.0 M, the

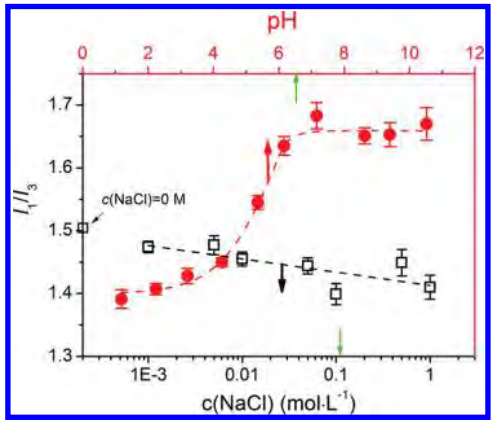

Figure 7. Plots of the I_1/I_3value vs pH (●) and salt concentration (□) for the SMA–Dopa52 micelles at a concentration of 1.0 mg·mL^{-1}. The concentration of pyrene was 3.75 × 10^{-8} mol·L^{-1}, λ_{ex} = 335 nm.

I_1/I_3 slightly decreases from 1.51 to 1.41, indicating that salt has little effect on the hydrophobicity of the SMA–Dopa micelles. In contrast, the I_1/I_3 value increases exponentially from 1.38 to 1.67 with an increase in pH from 1.23 to 6.16 and then slightly fluctuates around 1.67 as the pH levels off at 6.16. The transition point, at ca. pH 6.5 in the plot of I_1/I_3 vs pH is identical to that in the plot of the micelle size vs pH shown in Figure 6a. The first significant increase in the I_1/I_3 indicates a

dx.doi.org/10.1021/la301605a | *Langmuir* 2012, 28, 9211–9222

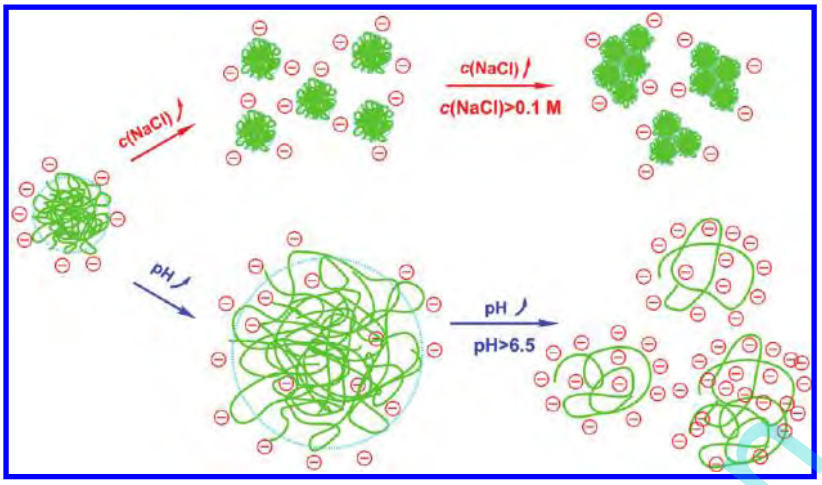

Figure 8. Schematic illustration of the structural transition of the SMA–Dopa52 micelles in response to pH and salinity changes.

dramatically enhanced polarity of the micelles that coincides with the swelling behavior of the micelles in response to increasing pH. Subsequent fluctuation of the I_1/I_3 value may be due to a balance between the progressive enhancement of polarity brought about by deprotonation and increased hydrophobic/hydrophilic phase interfacial area brought about by disintegration of the micelles. Note that the lowest I_1/I_3 value is found by lowering the pH to 1.37 and is smaller than that found by adding salt concentrations above 0.1 M, despite flocculation of the micelles occurring under both conditions. The hydrophobicity of the micelles under the former conditions is greater than that of the latter.

To aide in the understanding of the structural transition of the SMA–Dopa52 micelles, Figure 8 shows a schematic illustration according to the experimental results and analysis.

3.4. Interfacial Behavior of SMA–Dopa52 Micelles.

Prior to studying the emulsifying characteristics of the SMA–Dopa52 micelles, the IFT of the toluene–water interface in response to pH changes was investigated. Figure 9 shows that the IFT ranges from ca. 8.8 mN·m^{-1} to ca. 22 mN·m^{-1}, lower than that of the pure toluene–water interface at ca. 36 mN·m^{-1}. Increasing pH elevates the IFT of the toluene–water interface stabilized by the SMA–Dopa52. This variation trend coincides with reports that the surface in tension of HSMA aqueous solutions at pH 3 was lower than that at pH 12.5, as determined by the Wilhelmy method by Garnier et al.[56] It seems likely that the increased deprotonation of the SMA–Dopa52 will decrease the adsorption of the SMA–Dopa52 at the toluene–water interface.

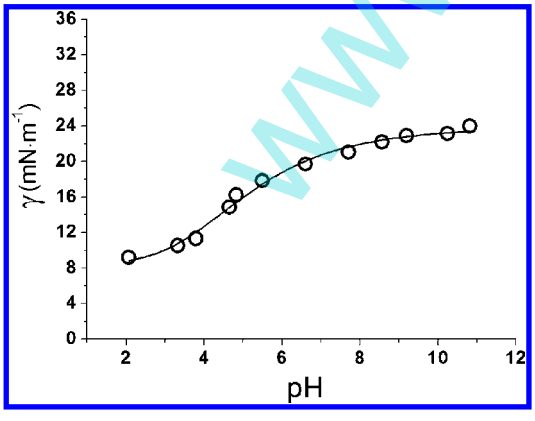

Figure 9. Influence of pH on the IFT at the toluene–water interface. The concentration of the SMA–Dopa52 micelles in aqueous solution is 2 mg·mL^{-1}, with 0.01 M NaCl. The pH was adjusted with HCl or NaOH aqueous solutions. Each pendant drop of micelle solution was immersed in toluene in a quartz cuvette, with aging for 0.5 h. T = 25 °C. The IFT of the pure toluene–water interface was determined to be 36 mN·m^{-1} prior to experiments.

The configuration of the emulsifier at the oil–water interface was further confirmed by SEM using an oil-phase solidification method, as shown in Figure 10. The structure of the micelles plays a crucial role in the oil–water interface behavior and the emulsification performance.

pH Influence. Comparing column a with column b in Figure 10, two typical manners of emulsification are shown. At pH 4.5,

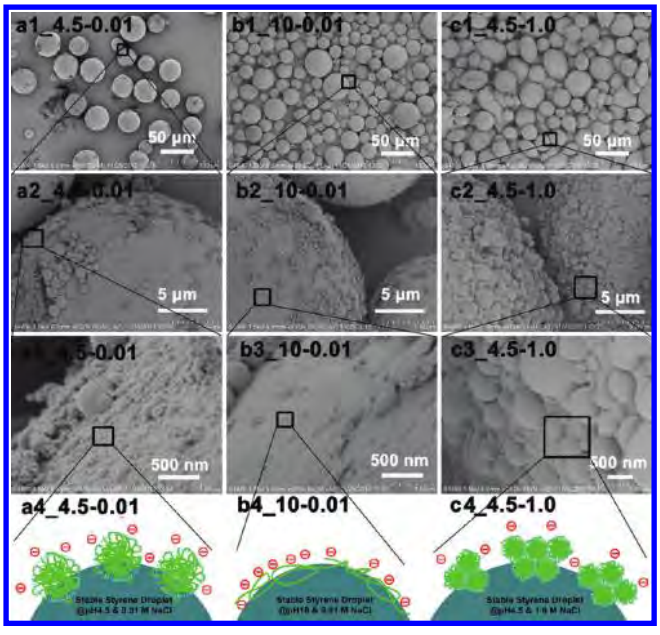

Figure 10. SEM images of polymerized styrene-in-water emulsions stabilized by the SMA–Dopa52 micelles under different conditions. For example, a1_4.5–0.01 represents the solidified emulsion droplets prepared at pH 4.5 with 0.01 M NaCl; the prefix a1–a3 represent the magnification of the samples, such as ×400, ×6K, and ×50K, except that c3 represents ×30K. The a4–c4 schematics illustrate the configuration of SMA–Dopa52 at the styrene–water interface under different conditions prior to polymerization.

dx.doi.org/10.1021/la301605a | *Langmuir* 2012, 28, 9211–9222

the stable SMA−Dopa52 micelles with moderately swollen structures maintain their spherical structures, with half of them embedding into the solidified oil droplets (PS beads), as shown in part a3 of Figure 10. The residual hemisphere indicates that the micelles could be well-wetted by both styrene and water. The good wettability of the micelles at the oil−water interface is also be supported by the lower interfacial tension (ca. 13.3 $mN{\cdot}m^{-1}$) of the toluene−water interface when stabilized by micelles relative to that (36 $mN{\cdot}m^{-1}$) of the pure toluene−water interface, as shown in Figure 9. Additionally, the spheres may provide steric hindrance as typical particulate emulsifiers, as illustrated in part a4 of Figure 10. As a comparison, at pH 10, there are many vacancies on the surface of the solidified oil droplets that appear to be smooth, as shown in part b3 of Figure 10. The vacancies indicate the fusion between the styrene−oil phase and the emulsifiers, which is actually a polymeric surfactant that works as illustrated in part b4 of Figure 10. Note that the mean size of the PS beads at pH 10 is smaller than that at pH 4.5, as shown by comparing part b1 with part a1 of Figure 10. Considering that the IFT at pH 10 (ca. 22 $mN{\cdot}m^{-1}$) was larger than that at pH 4.5 (ca. 13.3 $mN{\cdot}m^{-1}$, Figure 9), it is unusual for a lower interfacial tension to lead to a larger emulsion droplet sizes. This result probably occurred because the formed styrene-in-water emulsion at pH 10 solidified before the emulsion reached its most thermodynamically stable state.

Due the lower pH value, the greater hydrophobicity of the micelles in Figure 7, and the lower interfacial tension of the toluene−water interface, we chose the micelles at pH 2 to stabilize the styrene−water interface to visualize the morphologies of the severely shrunken micelles. Unfortunately, during the polymerization process, an oil phase separation occurred, suggesting that the styrene-in-water Pickering emulsion formed at pH 2 was unstable to the thermal stimulus generated by the polymerization. The phase separation may be due to the attraction overcoming the repulsion of the shrunken micelles adsorbed on the surface of neighboring styrene droplets, in spite of their steric hindrance.

Salinity Influence. By comparison of column a with column c in Figure 10, there are two typical Pickering emulsions stabilized by SMA−Dopa52 micelles with both salinities at pH 4.5. Figure 10 c2 and c3 shows the PS beads covered by 0.5−1.0-μm-sized particles, which were prepared from the styrene-in-water emulsion stabilized by SMA−Dopa52 micelles with 1.0 M NaCl. Because micelles shrink and flocculate as salinity increases from 0.01 to 1.0 M, we hypothesize that the larger particles at the styrene−water interface are the flocs of the shrunken primary SMA−Dopa52 micelles, as schematically represented in part c4 of Figure 10. Each floc acts as a single, large particulate emulsifier. Meanwhile, the floc emulsifiers are spherical and smooth on the surface of the PS beads, as shown in part c3 of Figure 10. This may result from the diffusion of styrene into the flocs at the styrene−water interface during polymerization. A similar phenomenon has been reported by Ge et al. in the synthesis of novel walnut-like multihollow polymer particles using a Pickering emulsion as a template.[77,78] Furthermore, the average size of the emulsion droplets stabilized by SMA−Dopa52 micelles with 1.0 M NaCl is larger than that with 0.01 M NaCl, as shown in parts c1 and a1 of Figure 10.

The configuration of the SMA−Dopa52 at the styrene−water interface depends on the aqueous phase prior to homogenization and also plays an important role in emulsion properties such as the emulsion droplet size and stability. Given the relationship between the particulate emulsifier size and the emulsion stability described by Binks et al. in detail,[43] the more rough the surface of the emulsion droplets (as can be seen in Figure 10), the more stable the emulsion.

3.5. Emulsifying Characterization of SMA−Dopa52 Micelles at Various pHs and Salinities. To investigate the influence of the micelle structures on the emulsifying performances, batches of stable toluene-in-water (i.e., o/w type, confirmed by drop test) emulsions were prepared using SMA−Dopa52 micelles at various pHs and salinities as emulsifiers. All emulsions were prepared under the same conditions with the exception of pH and salinity. All prepared emulsions were creamed without oil separation (i.e., all of the oil-phase was incorporated in the creaming because of the tensio-activity of the SMA−Dopa52 at each configuration).

The emulsions are characterized in terms of emulsifying efficiency and stability. In the present study, the total toluene−water interfacial area (S) of the emulsion products depends on the efficiency of the SMA−Dopa. The physical significance of S is similar to the apparent interfacial area per particle (S_{app}) for Pickering emulsions, as reported by Tilton et al.,[30] as well as the coverage used for emulsion stabilized by bacterial cellulose nanocrystals emulsifier by others.[70]

$$S = 4\pi R^2 \cdot \frac{3V_{oil}}{4\pi R^3} = \frac{3V_{oil}}{R} \quad (1)$$

where R is the average oil droplets radius and V_{oil} the volume of oil incorporated in the creaming layer. No oil separated out, indicating that V_{oil} is a constant. Thus, S is inversely dependent on the average oil droplet size, namely, that the smaller mean size of the emulsion droplets, the higher emulsifying efficiency. The assessment of the stability of the emulsion also depends on the variation of the size of the emulsion droplets with various placement durations under quiescence condition.

Salinity Influence. Figure 11 shows the influence of the salinity on the emulsions stabilized by SMA−Dopa52 micelles. There is a significant kick point in the size of the emulsion

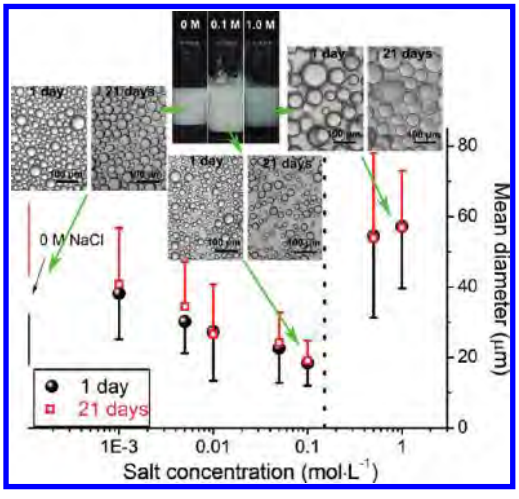

Figure 11. Influence of salinity on the toluene-in-water emulsion droplets under quiescent conditions with different placement durations: 1 day and 21 days after homogenization. The batch of emulsions (1:1 by volume) was stabilized by 2 $mg{\cdot}mL^{-1}$ SMA−Dopa52 micelles at pH 4.5 with various salt concentrations. The total volume was 10 mL. The mean diameter was counted with more than 600 emulsion droplets.

droplets in response to salinity changes, in line with the point where flocculation of SMA−Dopa52 micelles occurred with salt concentrations exceeding 0.1 M. Before the kick point, the size of the emulsion droplets decreases with increasing salinity. This decrease indicates that the emulsifying efficiency is enhanced by the addition of salt. Recalling the increase in the apparent zeta potential and the slight increase in hydrophobicity of the micelles with increasing salinity, we postulate that the enhanced efficiency can be contributed to a greater micelle migration from the aqueous phase to the toluene-in-water interface. The increased migration can be demonstrated by the increased transparency of the continuous aqueous phase of the emulsions with 0.1 M salt compared to that with no salt. This phenomenon is consistent with our previous report.[21] In spite of a higher number of micelles being incorporated into the creamy emulsion phase, the size of the emulsion droplets abruptly increases for salinities exceeding 0.1 M. This increase in size provides further evidence of (1) the inevitable formation of flocs of shrunken primary colloidal particles and (2) the floc emulsifier resulting in the reduction of the emulsifier concentration at the oil−water interface, as supported by Figure 10a,c. Note that there is little variation in the emulsion droplet size with 21 day placement compared to that with 1 day, indicating the excellent stability of the emulsions. In the absence of salt, a slight coalescence and Ostwald ripening occurred, probably due to the relatively swollen structure of the SMA−Dopa52 micelles at pH 4.5 without salt.

pH Influence. Figure 12 shows the influence of the pH on the emulsion droplet size. One day after homogenization, the size of the emulsion droplets decreases with increasing pH in the range 1−6 and remains constant thereafter. The transition point (ca. pH 6.5) is identical to the pH at which the disassociation of extremely swollen SMA−Dopa52 micelles occurs in aqueous solution. It is interesting to note that the emulsion droplets become larger after 21 days for pHs above the transition point.

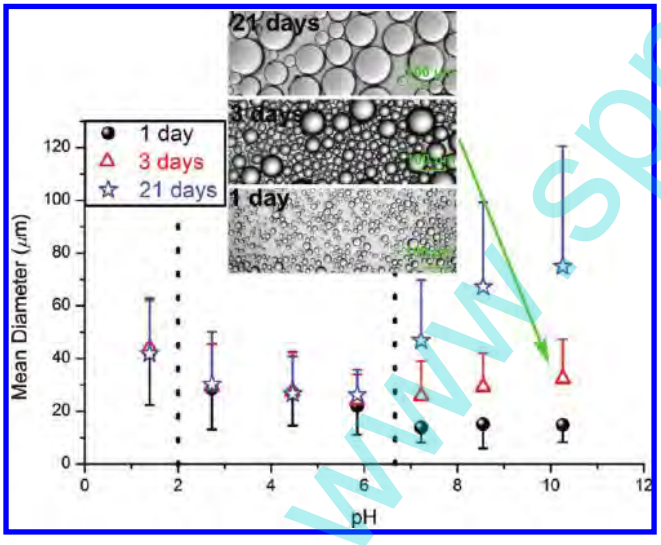

Figure 12. Influence of pH on the toluene-in-water emulsion droplets under quiescent conditions with different placement durations: 1 day, 3 days, and 21 days after homogenization. The batch of emulsions (1:1 by volume) was stabilized by 2 mg·mL^{-1} SMA−Dopa52 micelles at various pHs with 10 mM NaCl. The total volume was 10 mL. The mean diameter was counted with more than 600 emulsion droplets.

The toluene-in-water emulsions at pHs above the transition point are stabilized by typical polymeric surfactants, according to the configuration of SMA−Dopa52 at the styrene−water interface at pH 10 as shown in Figure 10b. Although there is no oil separation, coalescence and Ostwald ripening progressively occur after homogenization, indicating the thermodynamically unstable state of the prepared emulsions. As a comparison, the emulsions at pHs below the transition point are stable to coalescence and ripening, as shown in Figure 12, due to the steric hindrance of the spherical structures of the SMA−Dopa52 micelles at the oil−water interface as shown in Figure 10a. The droplet sizes of the emulsions for pHs ranging from 2 to 6 is smaller than that at pH 1.39, suggesting that micelles with moderately swollen structures possess higher emulsifying efficiencies than those with shrunken structures. Additionally, recalling that the emulsions stabilized by micelles at pH < 2 are unstable to thermal stimulus during styrene oil-phase polymerization, the emulsions at 2 < pH < 6 combine the advantages of the stability of emulsions stabilized by solid particulate emulsifiers and the efficiency of emulsions stabilized by polymeric surfactants. The excellent emulsifying performance of the SMA−Dopa52 micelles at 2 < pH < 6 is similar to polymer-graft nanoparticles[30,31] and lightly cross-linked microgel particles,[42,45] originating from their moderately swollen structure.

Noteworthy, there are light coalescence occurred among the emulsion droplets at pH 5.8 with long-term placement. The probable reason is that the micelles with very swollen structure would decrease its stability at the oil−water interface because of the wetting and dissolution brought by oil phase. There is a balance between the efficiency and stability. Hence, lightly cross-linking would be a desirable tool to tackle the challenge that maintaining both the stability and efficiency.[35,79]

CONCLUSION

A particulate emulsifier was designed and prepared via self-assembly based on a new type of amphiphilic random copolymer, SMA−Dopa. SMA−Dopa was synthesized via an aminolysis reaction between dopamine and SMA. Dopamine moieties facilitate the self-assembly of the SMA−Dopa in selective solvents into stable micelles and increase the adsorption of the SMA−Dopa at the oil−water interface. In addition to the chemical structure of the SMA−Dopa, the influence of postnatal stimulus (i.e., salt, pH) on the micellar structure and, in turn, on the emulsifying performance of the micelles as emulsifiers was characterized. The structural transition of the self-assembled SMA−Dopa52 micelles in response to pH and salinity changes were confirmed by TEM, AFM, DLS, aqueous electrophoresis techniques, potentiometric titration, and the fluorescence pyrene probe method. Micelles shrunk with increasing salinity, and flocculation of the shrunken primary micelles occurred for salt concentrations exceeding 0.1 M. The micelles swelled with increasing pH, and the disassociation of the SMA−Dopa52 micelles occurred for pH levels above approximately 6.5. The structure of the micelles plays a crucial role on the oil−water interfacial performance. Micelles with various structures were used as emulsifiers to adsorb at the styrene-in-water and toluene-in-water interfaces. The emulsifying characteristics demonstrated that self-assembled SMA−Dopa52 micelles with moderately swollen structures (at 2 < pH < 6) combine the advantages of solid particulate emulsifiers and polymeric surfactants, possessing excellent emulsifying efficiencies and good emulsion stability.

dx.doi.org/10.1021/la301605a | *Langmuir* 2012, 28, 9211−9222

The addition of salt was able to further enhance the emulsification performance of the SMA−Dopa52 micelles. Moreover, the structural transition of the self-assembled micelles, accompanied by the emulsification performance changes, illuminates the transition from the emulsifying manner of polymeric surfactants to that of polymeric particulate emulsifiers. Therefore, the self-assembled micelles as model polymeric particulate emulsifiers may aid in future studies of the surface activity of polymeric surfactants and help to explain the emulsification mechanism of the stimuli-responsive polymeric particulate emulsifiers, including sterically stabilized polystyrene latexes,[36−38] polymeric microgels,[35,45,46,79] and nanoparticles with grafted polymer brushes.[30,32] These results help in understanding the challenging areas where polymeric surfactants and particulate emulsifiers cooperate,[54,55] such as in the cosmetic and food industries.

■ ASSOCIATED CONTENT

Supporting Information

Synthesis and characterization of the SMA−Dopa polymers; the synthesis and emulsification characterizations of dopamine-modified hyaluronic acid; the conductometric and pH titrations of the SMA−Dopa52 micelles. This material is available free of charge via the Internet at http://pubs.acs.org.

■ AUTHOR INFORMATION

Notes

The authors declare no competing financial interest.

■ ACKNOWLEDGMENTS

We acknowledge financial support from the National Nature Science Foundation of China (NSFC) (under Grants Nos. 20974041, 21174056), and the Fundamental Research Funds for the Central Universities (JUDCF09007).

■ REFERENCES

(1) Zhang, L.; Eisenberg, A. Multiple Morphologies of "Crew-Cut" Aggregates of Polystyrene-b-poly(acrylic acid) Block Copolymers. *Science* **1995**, *268* (5218), 1728−1731.

(2) Liu, X.; Kim, J.-S.; Wu, J.; Eisenberg, A. Bowl-Shaped Aggregates from the Self-Assembly of an Amphiphilic Random Copolymer of Poly(styrene-co-methacrylic acid). *Macromolecules* **2005**, *38* (16), 6749−6751.

(3) Chen, D.; Jiang, M. Strategies for Constructing Polymeric Micelles and Hollow Spheres in Solution via Specific Intermolecular Interactions. *Acc. Chem. Res.* **2005**, *38* (6), 494−502.

(4) Jiang, J.; Shu, Q.; Chen, X.; Yang, Y.; Yi, C.; Song, X.; Liu, X.; Chen, M. Photoinduced Morphology Switching of Polymer Nano-aggregates in Aqueous Solution. *Langmuir* **2010**, *26* (17), 14247−14254.

(5) Tian, F.; Yu, Y.; Wang, C.; Yang, S. Consecutive Morphological Transitions in Nanoaggregates Assembled from Amphiphilic Random Copolymer via Water-Driven Micellization and Light-Triggered Dissociation. *Macromolecules* **2008**, *41* (10), 3385−3388.

(6) Yu, S.; Azzam, T.; Rouiller, I.; Eisenberg, A. "Breathing" Vesicles. *J. Am. Chem. Soc.* **2009**, *131* (30), 10557−10566.

(7) Yu, Y.; Eisenberg, A. Control of Morphology through Polymer−Solvent Interactions in Crew-Cut Aggregates of Amphiphilic Block Copolymers. *J. Am. Chem. Soc.* **1997**, *119* (35), 8383−8384.

(8) Wei, C.; Guo, J.; Wang, C. Dual Stimuli-Responsive Polymeric Micelles Exhibiting "AND" Logic Gate for Controlled Release of Adriamycin. *Macromol. Rapid Commun.* **2011**, *32* (5), 451−455.

(9) Blanazs, A.; Armes, S. P.; Ryan, A. J. Self-Assembled Block Copolymer Aggregates: From Micelles to Vesicles and their Biological Applications. *Macromol. Rapid Commun.* **2009**, *30* (4−5), 267−277.

(10) Qu, T.; Wang, A.; Yuan, J.; Gao, Q. Preparation of an amphiphilic triblock copolymer with pH- and thermo-responsiveness and self-assembled micelles applied to drug release. *J. Colloid Interface Sci.* **2009**, *336* (2), 865−871.

(11) Wang, T.; Li, M.; Gao, H.; Wu, Y. Nanoparticle carriers based on copolymers of poly(ε-caprolactone) and hyperbranched polymers for drug delivery. *J. Colloid Interface Sci.* **2011**, *353* (1), 107−115.

(12) Wang, Y.; Han, P.; Xu, H.; Wang, Z.; Zhang, X.; Kabanov, A. V. Photocontrolled Self-Assembly and Disassembly of Block Ionomer Complex Vesicles: A Facile Approach toward Supramolecular Polymer Nanocontainers. *Langmuir* **2009**, *26* (2), 709−715.

(13) Ge, Z.; Xie, D.; Chen, D.; Jiang, X.; Zhang, Y.; Liu, H.; Liu, S. Stimuli-Responsive Double Hydrophilic Block Copolymer Micelles with Switchable Catalytic Activity. *Macromolecules* **2007**, *40* (10), 3538−3546.

(14) Li, Z.; Ding, J.; Day, M.; Tao, Y. Molecularly Imprinted Polymeric Nanospheres by Diblock Copolymer Self-Assembly. *Macromolecules* **2006**, *39* (7), 2629−2636.

(15) Hu, J.; Li, C.; Liu, S. Hg^{2+}-Reactive Double Hydrophilic Block Copolymer Assemblies as Novel Multifunctional Fluorescent Probes with Improved Performance. *Langmuir* **2009**, *26* (2), 724−729.

(16) Yang, Y.; Yi, C.; Luo, J.; Liu, R.; Liu, J.; Jiang, J.; Liu, X. Glucose sensors based on electrodeposition of molecularly imprinted polymeric micelles: A novel strategy for MIP sensors. *Biosens. Bioelectron.* **2011**, *26* (5), 2607−2612.

(17) Cho, J.; Hong, J.; Char, K.; Caruso, F. Nanoporous Block Copolymer Micelle/Micelle Multilayer Films with Dual Optical Properties. *J. Am. Chem. Soc.* **2006**, *128* (30), 9935−9942.

(18) Fujii, S.; Cai, Y.; Weaver, J. V. M; Armes, S. P. Syntheses of Shell Cross-Linked Micelles Using Acidic ABC Triblock Copolymers and Their Application as pH-Responsive Particulate Emulsifiers. *J. Am. Chem. Soc.* **2005**, *127* (20), 7304−7305.

(19) Yang, Y.; Yi, C.; Wang, Y.; Jiang, J.; Liu, X. Self-Assembly and Emulsification of the Alternating Copolymer P(St-*alt*-Ma-Dopa). *Acta Phys. Chim. Sin.* **2009**, *25* (11), 2225−2231.

(20) Liu, X.; Wang, Y.; Yi, C.; Feng, Y.; Jiang, J.; Cui, Z.; Chen, M. Self-assembly and Emulsification Behavior of Photo-sensitive P(St/CS-*alt*-MA) Copolymer. *Acta Chim. Sin.* **2009**, *67* (5), 447−452.

(21) Liu, X.; Yi, C.; Zhu, Y.; Yang, Y.; Jiang, J.; Cui, Z.; Jiang, M. Pickering emulsions stabilized by self-assembled colloidal particles of copolymers of P(St-alt-MAn)-co-P(VM-alt-MAn). *J. Colloid Interface Sci.* **2010**, *351* (2), 315−322.

(22) Pickering, S. U. Emulsions. *J. Chem. Soc., Trans.* **1907**, *91*, 2001−2021.

(23) Ramsden, W. Separation of Solids in the Surface-Layers of Solutions and 'Suspensions' (Observations on Surface-Membranes, Bubbles, Emulsions, and Mechanical Coagulation). *Proc. R. Soc. Lond.* **1903**, *72*, 156−164.

(24) Zhang, K.; Wu, W.; Guo, K.; Chen, J.; Zhang, P. Synthesis of Temperature-Responsive Poly(N-isopropyl acrylamide)/Poly(methyl methacrylate)/Silica Hybrid Capsules from Inverse Pickering Emulsion Polymerization and Their Application in Controlled Drug Release. *Langmuir* **2010**, *26* (11), 7971−7980.

(25) Kargar, M.; Fayazmanesh, K.; Alavi, M.; Spyropoulos, F.; Norton, I. T. Investigation into the potential ability of Pickering emulsions (food-grade particles) to enhance the oxidative stability of oil-in-water emulsions. *J. Colloid Interface Sci.* **2012**, *366* (1), 209−215.

(26) Crossley, S.; Faria, J.; Shen, M.; Resasco, D. E. Solid Nanoparticles that Catalyze Biofuel Upgrade Reactions at the Water/Oil Interface. *Science* **2010**, *327* (5961), 68−72.

(27) Dinsmore, A. D.; Hsu, M. F.; Nikolaides, M. G.; Marquez, M.; Bausch, A. R.; Weitz, D. A. Colloidosomes: Selectively Permeable Capsules Composed of Colloidal Particles. *Science* **2002**, *298* (5595), 1006−1009.

(28) Ikem, V. O.; Menner, A.; Bismarck, A. High Internal Phase Emulsions Stabilized Solely by Functionalized Silica Particles. *Angew. Chem., Int. Ed.* **2008**, *47* (43), 8277−8279.

(29) Cauvin, S.; Colver, P. J.; Bon, S. A. F. Pickering Stabilized Miniemulsion Polymerization: Preparation of Clay Armored Latexes. *Macromolecules* **2005**, *38* (19), 7887−7889.
(30) Sarbu, T.; Sirk, K.; Lowry, G. V.; Matyjaszewski, K.; Tilton, R. D. Oil-in-Water Emulsions Stabilized by Highly Charged Polyelectrolyte-Grafted Silica Nanoparticles. *Langmuir* **2005**, *21* (22), 9873−9878.
(31) Saigal, T.; Dong, H.; Matyjaszewski, K.; Tilton, R. D. Pickering Emulsions Stabilized by Nanoparticles with Thermally Responsive Grafted Polymer Brushes. *Langmuir* **2010**, *26* (19), 15200−15209.
(32) Wu, Y.; Zhang, C.; Qu, X.; Liu, Z.; Yang, Z. Light-Triggered Reversible Phase Transfer of Composite Colloids. *Langmuir* **2010**, *26* (12), 9442−9448.
(33) Tan, K. Y.; Gautrot, J. E.; Huck, W. T. S. Formation of Pickering Emulsions Using Ion-Specific Responsive Colloids. *Langmuir* **2010**, *27* (4), 1251−1259.
(34) Binks, B. P.; Rodrigues, J. A. Inversion of Emulsions Stabilized Solely by Ionizable Nanoparticles. *Angew. Chem., Int. Ed.* **2005**, *44* (3), 441−444.
(35) Dupin, D.; Armes, S. P.; Connan, C.; Reeve, P.; Baxter, S. M. How Does the Nature of the Steric Stabilizer Affect the Pickering Emulsifier Performance of Lightly Cross-Linked, Acid-Swellable Poly(2-vinylpyridine) Latexes? *Langmuir* **2007**, *23* (13), 6903−6910.
(36) Binks, B. P.; Murakami, R.; Armes, S. P.; Fujii, S. Temperature-Induced Inversion of Nanoparticle-Stabilized Emulsions. *Angew. Chem., Int. Ed.* **2005**, *44* (30), 4795−4798.
(37) Binks, B. P.; Murakami, R.; Armes, S. P.; Fujii, S.; Schmid, A. pH-Responsive Aqueous Foams Stabilized by Ionizable Latex Particles. *Langmuir* **2007**, *23* (17), 8691−8694.
(38) Read, E. S.; Fujii, S.; Amalvy, J. I.; Randall, D. P.; Armes, S. P. Effect of Varying the Oil Phase on the Behavior of pH-Responsive Latex-Based Emulsifiers: Demulsification versus Transitional Phase Inversion. *Langmuir* **2004**, *20* (18), 7422−7429.
(39) Fujii, S.; Suzaki, M.; Armes, S. P.; Dupin, D.; Hamasaki, S.; Aono, K.; Nakamura, Y. Liquid Marbles Prepared from pH-Responsive Sterically Stabilized Latex Particles. *Langmuir* **2011**, *27* (13), 8067−8074.
(40) Li, Z.; Ming, T.; Wang, J.; Ngai, T. High Internal Phase Emulsions Stabilized Solely by Microgel Particles. *Angew. Chem., Int. Ed.* **2009**, *48* (45), 8490−8493.
(41) Brugger, B.; Rosen, B. A.; Richtering, W. Microgels as Stimuli-Responsive Stabilizers for Emulsions. *Langmuir* **2008**, *24* (21), 12202−12208.
(42) Brugger, B.; Richtering, W. Emulsions Stabilized by Stimuli-Sensitive Poly(N-isopropylacrylamide)-co-Methacrylic Acid Polymers: Microgels versus Low Molecular Weight Polymers. *Langmuir* **2008**, *24* (15), 7769−7777.
(43) Binks, B. P. Particles as surfactants——similarities and differences. *Curr. Opin. Colloid Interface Sci.* **2002**, *7*, 21−41.
(44) Aveyard, R.; Binks, B. P.; Clint, J. H. Emulsions stabilised solely by colloidal particles. *Adv. Colloid Interface Sci.* **2003**, *100−102*, 503−546.
(45) Ngai, T.; Behrens, S. H.; Auweter, H. Novel emulsions stabilized by pH and temperature sensitive microgels. *Chem. Commun.* **2005**, *3*, 331−333.
(46) Ngai, T.; Auweter, H.; Behrens, S. H. Environmental Responsiveness of Microgel Particles and Particle-Stabilized Emulsions. *Macromolecules* **2006**, *39* (23), 8171−8177.
(47) Suzuki, D.; Tsuji, S.; Kawaguchi, H. Janus Microgels Prepared by Surfactant-Free Pickering Emulsion-Based Modification and Their Self-Assembly. *J. Am. Chem. Soc.* **2007**, *129* (26), 8088−8089.
(48) Wang, M.; Braun, H.-G.; Meyer, E. Patterning of Polymeric/Inorganic Nanocomposite and Nanoparticle Layers. *Chem. Mater.* **2002**, *14* (11), 4812−4818.
(49) Peng, M.; Liao, Z.; Zhu, Z.; Guo, H. A Simple Polymerizable Polysoap Greatly Enhances the Grafting Efficiency of the "Grafting-to" Functionalization of Multiwalled Carbon Nanotubes. *Macromolecules* **2010**, *43* (23), 9635−9644.
(50) Lazzara, T. D.; Bourret, G. R.; Lennox, R. B.; van de Ven, T. G. M. Polymer Templated Synthesis of AgCN and Ag Nanowires. *Chem. Mater.* **2009**, *21* (10), 2020−2026.
(51) Lai, C.-T.; Hong, J.-L. Role of Concentration on the Formulation of Zinc Oxide Nanorods from Poly(styrene-alt-maleic acid) Template. *J. Phys. Chem. C* **2009**, *113* (43), 18578−18583.
(52) Benoit, D. S. W.; Henry, S. M.; Shubin, A. D.; Hoffman, A. S.; Stayton, P. S. pH-Responsive Polymeric siRNA Carriers Sensitize Multidrug Resistant Ovarian Cancer Cells to Doxorubicin via Knockdown of Polo-like Kinase 1. *Mol. Pharmaceutics* **2010**, *7* (2), 442−455.
(53) Henry, S. M.; El-Sayed, M. E. H.; Pirie, C. M.; Hoffman, A. S.; Stayton, P. S. pH-Responsive Poly(styrene-alt-maleic anhydride) Alkylamide Copolymers for Intracellular Drug Delivery. *Biomacromolecules* **2006**, *7* (8), 2407−2414.
(54) Bouyer, E.; Mekhloufi, G.; Potier, I. L.; Kerdaniel, T. d. F. d.; Grossiord, J.-L.; Rosilio, V.; Agnely, F. Stabilization mechanism of oil-in-water emulsions by *β*-lactoglobulin and gum arabic. *J. Colloid Interface Sci.* **2011**, *354* (2), 467−477.
(55) Sugita, N.; Nomura, S.; Kawaguchi, M. Rheological and interfacial properties of silicone oil emulsions prepared by polymer pre-adsorbed onto silica particles. *Colloids Surf., A* **2008**, *328* (1−3), 114−122.
(56) Garnier, G.; Duskova-Smrckova, M.; Vyhnalkova, R.; van de Ven, T. G. M.; Revol, J.-F. Association in Solution and Adsorption at an Air−Water Interface of Alternating Copolymers of Maleic Anhydride and Styrene. *Langmuir* **2000**, *16* (8), 3757−3763.
(57) Malardier-Jugroot, C. Novel self-assembly of an alternating copolymer into nanotubes: Theoretical investigation and experimental characterisation; McGill: Montreal, Canada, 2004.
(58) Malardier-Jugroot, C.; van de Ven, T. G. M.; Whitehead, M. A. Study of the water conformation around hydrophilic and hydrophobic parts of styrene-maleic anhydride. *THEOCHEM* **2004**, *679* (3), 171−177.
(59) Malardier-Jugroot, C.; van de Ven, T. G. M.; Cosgrove, T.; Richardson, R. M.; Whitehead, M. A. Novel Self-Assembly of Amphiphilic Copolymers into Nanotubes: Characterization by Small-Angle Neutron Scattering. *Langmuir* **2005**, *21* (22), 10179−10187.
(60) Malardier-Jugroot, C.; van de Ven, T. G. M.; Whitehead, M. A. Linear Conformation of Poly(styrene-alt-maleic anhydride) Capable of Self-Assembly: A Result of Chain Stiffening by Internal Hydrogen Bonds. *J. Phys. Chem. B* **2005**, *109* (15), 7022−7032.
(61) Lee, H.; Dellatore, S. M.; Miller, W. M.; Messersmith, P. B. Mussel-Inspired Surface Chemistry for Multifunctional Coatings. *Science* **2007**, *318* (5849), 426−430.
(62) Lee, B. P.; Messersmith, P. B.; Israelachvili, J. N.; Waite, J. H. Mussel-Inspired Adhesives and Coatings. *Annu. Rev. Mater. Res.* **2011**, *41* (1), 99−132.
(63) Lee, Y.; Lee, H.; Kim, Y. B.; Kim, J.; Hyeon, T.; Park, H.; Messersmith, P. B.; Park, T. G. Bioinspired Surface Immobilization of Hyaluronic Acid on Monodisperse Magnetite Nanocrystals for Targeted Cancer Imaging. *Adv. Mater.* **2008**, *20* (21), 4154−4157.
(64) Shultz, M. D.; Reveles, J. U.; Khanna, S. N.; Carpenter, E. E. Reactive Nature of Dopamine as a Surface Functionalization Agent in Iron Oxide Nanoparticles. *J. Am. Chem. Soc.* **2007**, *129* (9), 2482−2487.
(65) Shalev, T.; Gopin, A.; Bauer, M.; Stark, R. W.; Rahimipour, S. Non-leaching antimicrobial surfaces through polydopamine bio-inspired coating of quaternary ammonium salts or an ultrashort antimicrobial lipopeptide. *J. Mater. Chem.* **2012**, *22* (5), 2026−2032.
(66) Yang, L.; Phua, S. L.; Teo, J. K. H.; Toh, C. L.; Lau, S. K.; Ma, J.; Lu, X. A Biomimetic Approach to Enhancing Interfacial Interactions: Polydopamine-Coated Clay as Reinforcement for Epoxy Resin. *ACS Appl. Mater. Interfaces* **2011**, *3* (8), 3026−3032.
(67) Jiang, J.; Zhu, L.; Zhu, L.; Zhu, B.; Xu, Y. Surface Characteristics of a Self-Polymerized Dopamine Coating Deposited on Hydrophobic Polymer Films. *Langmuir* **2011**, *27* (23), 14180−14187.

(68) Lianos, P. Fluorescence probe study of the interaction between pyrene and microemulsion-polymerized styrene. *J. Phys. Chem.* **1982**, *86* (11), 1935−1937.
(69) Wilhelm, M.; Zhao, C. L.; Wang, Y.; Xu, R.; Winnik, M. A.; Mura, J. L.; Riess, G.; Croucher, M. D. Poly(styrene-ethylene oxide) block copolymer micelle formation in water: a fluorescence probe study. *Macromolecules* **1991**, *24* (5), 1033−1040.
(70) Kalashnikova, I.; Bizot, H.; Cathala, B.; Capron, I. New Pickering Emulsions Stabilized by Bacterial Cellulose Nanocrystals. *Langmuir* **2011**, *27* (12), 7471−7479.
(71) Gliemann, H.; Mei, Y.; Ballauff, M.; Schimmel, T. Adhesion of Spherical Polyelectrolyte Brushes on Mica: An in Situ AFM Investigation. *Langmuir* **2006**, *22* (17), 7254−7259.
(72) Garrett, E. R.; Guile, R. L. Potentiometric Titrations of a Polydicarboxylic Acid: Maleic Acid-Styrene Copolymer. *J. Am. Chem. Soc.* **1951**, *73* (10), 4533−4535.
(73) Snowden, M. J.; Chowdhry, B. Z.; Vincent, B.; Morris, G. E. Colloidal copolymer microgels of N-isopropylacrylamide and acrylic acid: pH, ionic strength and temperature effects. *J. Chem. Soc., Faraday Trans.* **1996**, *92* (24), 5013−5016.
(74) Zhang, G.; Li, X.; Jiang, M.; Wu, C. Model System for Surfactant-free Emulsion Copolymerization of Hydrophobic and Hydrophilic Monomers in Aqueous Solution. *Langmuir* **2000**, *16* (24), 9205−9207.
(75) Zhang, G.; Liu, L.; Zhao, Y.; Ning, F.; Jiang, M.; Wu, C. Self-Assembly of Carboxylated Poly(styrene-b-ethylene-co-butylene-b-styrene) Triblock Copolymer Chains in Water via a Microphase Inversion. *Macromolecules* **2000**, *33* (17), 6340−6343.
(76) Kalyanasundaram, K.; Thomas, J. K. Environmental effects on vibronic band intensities in pyrene monomer fluorescence and their application in studies of micellar systems. *J. Am. Chem. Soc.* **1977**, *99* (7), 2039−2044.
(77) He, X.; Ge, X.; Liu, H.; Wang, M.; Zhang, Z. Synthesis of Cagelike Polymer Microspheres with Hollow Core/Porous Shell Structures by Self-Assembly of Latex Particles at the Emulsion Droplet Interface. *Chem. Mater.* **2005**, *17* (24), 5891−5892.
(78) Ge, X.; Wang, M.; Wang, H.; Yuan, Q.; Ge, X.; Liu, H.; Tang, T. Novel Walnut-like Multihollow Polymer Particles: Synthesis and Morphology Control. *Langmuir* **2009**, *26* (3), 1635−1641.
(79) Fujii, S.; Read, E. S.; Binks, B. P.; Armes, S. P. Stimulus-Responsive Emulsifiers Based on Nanocomposite Microgel Particles. *Adv. Mater.* **2005**, *17* (8), 1014−1018.